Journal of Nuclear Materials 392 (2009) 519–524

Contents lists available at ScienceDirect

Journal of Nuclear Materials

journal homepage: www.elsevier.com/locate/jnucmat

Immobilization of selenate by iron in aqueous solution under anoxic conditions and the influence of uranyl

Anders Puranen [a,*], Mats Jonsson [a], Rainer Dähn [b], Daqing Cui [c]

[a] KTH Chemical Science and Engineering, Nuclear Chemistry, Royal Institute of Technology, Se 100 44 Stockholm, Sweden
[b] Laboratory for Waste Management, Paul Scherrer Institut, Villigen, CH-5232, Switzerland
[c] Hot Cell Lab, Studsvik Nuclear AB, 71182 Nyköping, Sweden

ARTICLE INFO

Article history:
Received 23 December 2008
Accepted 21 April 2009

ABSTRACT

In proposed high level radioactive waste repositories a large part of the spent nuclear fuel (SNF) canisters are commonly composed of iron. Selenium is present in spent nuclear fuel as a long lived fission product. This study investigates the influence of iron on the uptake of dissolved selenium in the form of selenate and the effect of the presence of dissolved uranyl on the above interaction of selenate. The iron oxide, and selenium speciation on the surfaces was investigated by Raman spectroscopy. X-ray Absorption Spectroscopy was used to determine the oxidation state of the selenium and uranium on the surfaces. Under the simulated groundwater conditions (10 mM NaCl, 2 mM $NaHCO_3$, <0.1 ppm O_2) the immobilized selenate was found to be reduced to oxidation states close to zero or lower and uranyl was found to be largely reduced to U(IV). The near simultaneous reduction of uranyl was found to greatly enhance the rate of selenate reduction. These findings suggest that the presence of uranyl being reduced by an iron surface could substantially enhance the rate of reduction of selenate under anoxic conditions relevant for a repository.

1. Introduction

^{79}Selenium exists as a fission product in spent nuclear fuel (SNF). Although the amount of selenium in SNF is comparatively small comprising ~0.001% of the fuel at the time of discharge, the long half life of ^{79}Se (reported in the range of 10^5–10^6 years, [1]), combined with its potentially high mobility and bioavailability makes it one of the key concerns in the safety assessment for a SNF repository. Selenium can exist as soluble selenate, Se(VI) and selenite Se(IV), as more sparingly soluble selenides, Se(-II) and Se(-I) or zero valent selenium. The selenate anion in particular is expected to be highly mobile due to the potential difficulty of immobilizing it under the conditions expected in a deep geological repository [2]. The Swedish spent nuclear fuel canister design, KBS-3 [3] consists of an outer copper cylinder surrounding an iron insert that holds the spent fuel. In common with several other canister designs a significant part of the canister will be composed of iron. In order for the SNF to be exposed to the groundwater the barrier function of the canister must fail. The iron will thereby come in contact with anoxic groundwater and corrode as the SNF matrix dissolves and releases fission products such as selenium. Iron and certain iron corrosion products have been shown to reduce and thus immobilize dissolved selenite and selenate [4–10]. To the best of our knowledge data on the immobilization of selenate by iron and the effect of uranyl present in solution is however scarce. Since SNF is composed of ~95% UO_2, a large amount of uranium would have to dissolve in order for the SNF matrix to release significant amounts of fission products such as ^{79}selenium. The effect of the presence of UO_2^{2+} or uranium dioxide on the immobilization of Se should consequently be investigated. Uranium present as uranyl cations (UO_2^{2+}), hydroxides or carbonate complexes could become immobilized and reduced on iron and iron corrosion products [11,12].

This study focuses on examining to what extent selenate immobilization by iron is affected by the presence of dissolved uranyl under anoxic conditions in simulated groundwater. Surface characterization was performed using Raman spectroscopy, SEM–EDS (Scanning Electron Microscopy Energy Dispersive X-ray Spectroscopy) and micro-XAS (X-ray Absorption Spectroscopy).

2. Materials and methods

Iron foils (Goodfellow 99.75%-Fe), 20 μm thick were cut inside a glove box (<0.1 ppm O_2) and polished to expose a fresh surface. The foils were then washed in distilled water to remove the polishing

* Corresponding author.
E-mail address: puranen@kth.se (A. Puranen).

0022-3115/$ - see front matter © 2009 Elsevier B.V. All rights reserved.
doi:10.1016/j.jnucmat.2009.04.016

residues. They were divided so that several small pieces gave a total area ~4 cm^2 per sample.

Three types of materials were prepared:

- N: polished iron foils with no precorrosion.
- P: precorroded foils. Polished iron foils were exposed to a solution of 0.42 mM U(VI) in a sealed glass vessel in the glove box. The concentration of dissolved uranium dropped to below 1 μM within days and a thick black precipitate formed. Over time the black corrosion products became more voluminous and loosely attached to the iron foil. The foils were left in the solution at ~25 °C for 300 days.
- UO_2: 1 g of UO_2 powder supplied from Westinghouse Atom AB.

Small subsamples of the materials were examined by Raman spectroscopy to identify the corrosion products.

2.1. Batch experiments

The conditions for the batch experiments are presented in Table 1.

Sample N-250Se represents selenate interaction with a fresh iron surface. In sample N-250Se/420U, a fresh iron surface is exposed to dissolved uranyl as well as selenate. Sample P-250Se is an iron foil that was precorroded with uranyl for a considerable time (300 days) prior to the addition of selenate. In sample P-250Se/420U the conditions are the same as in P-250Se except for a second addition of uranyl together with the addition of selenate. Sample UO_2–250Se is a bulk UO_2 powder sample exposed to selenate with no iron. In the experiments the sample materials were exposed to solutions containing non radioactive selenate under anoxic conditions in simulated groundwater (10 mM NaCl, 2 mM $NaHCO_3$, Ar + 0.03% CO_2).

A reference solution containing only selenate, uranyl and the simulated groundwater was also included.

Plastic bottles with 50 ml solution were used. All solutions were prepared inside the glove box (<0.1 ppm O_2, Ar + 0.03% CO_2) from degassed Milli-Q deionized water (18 MΩ). Uranylnitrate (Kebo, Pro analysi) was used to prepare the uranyl solutions. The selenate used (Na_2SeO_4, Alfa Aesar, 99.8%) for the solutions was analyzed iodometrically to test for any selenite contamination, of which none could be detected.

The selenium and uranium concentrations in solutions were measured by ICP–OES (Inductively Coupled Plasma Optical Emission Spectrometry).

Two small subsamples were removed from each solution, briefly dipped in deionized water followed by a quick immersion in ethanol in the glove box. Analysis of the rinsing solutions did not indicate any removal of Se or U by these steps. After drying the subsamples were either cast in epoxy and polished or fixated on kapton tape for SEM–EDS and XAS analysis. The samples for Raman analysis were sealed under a thin cover glass.

2.2. X-ray spectroscopy

Micro-XAS spectroscopy and fluorescence microprobe mapping was performed at the micro-XAS beamline at the Swiss Light Source (SLS) [13]. The beam size was ~2 × 6 μm^2. Commercial liquid sodiumselenate, selenite, solid gray elemental Se, ferroselite and dioctyldiselenide were used as Se references. The dioctyldiselenide, Se(-I) reference prepared according to Syper and Mlochowski [14] and confirmed by NMR was kindly provided by Professor Lars Engman at Uppsala University, Sweden. For uranium uranylnitrate and UO_2 references were used. Prior to transport to the beamline the samples were sealed (in the glove box) in a double air tight container with freshly regenerated oxygen scavenging copper pellets in the outer compartment of the container. The colour of the copper pellets indicated no intrusion of oxygen prior to the XAS analysis. Multiple micro XANES spectra were recorded for each region of interest and the first and last of each series was compared to check for possible redox reactions induced by the high photon flux of the synchrotron beam, of which no indication was found. The U or Se in the dried and encapsulated samples did not appear to be sensitive to oxidation by air or by redox effects while being handled at the beamline over the course of a few days and repeated beam exposures. Data averaging (three to five spectra from each spot), background correction and normalization was performed in the program WINXAS [15]. All spectra were collected at room temperature.

2.3. Raman microscopy

Samples were transferred out of the glove box for immediate investigation by Raman microscopy. A Renishaw 1000 system with a 633 nm Spectra Physics model 127 laser was used. The spectra were recorded at room temperature using 20× and 80× magnification, corresponding to a spatial resolution of 5 μm or less. Cosmic ray suppression was employed. No effects of laser induced decomposition of the samples were observed.

3. Results and discussion

3.1. Characterization of the uranyl precorroded layers

The Raman spectra obtained for the iron foil precorroded in uranyl, the bulk UO_2 powder used in this work; magnetite and uranyl nitrate reference powders are shown in Fig. 1.

The major band at 670 cm^{-1} on the iron foil agrees with reported data for magnetite [16], indicating magnetite as the dominating species on the uranyl precorroded iron surfaces. Magnetite is believed to be a likely major corrosion product of iron corroding under anoxic groundwater conditions [17,18]. It must be noted that the probing depth of the Raman analysis is estimated to be in the range of 0.5–1 μm [18]. A thin corrosion film of a different composition on the surface of the material could thus remain undetected if the bulk of the underlaying corrosion layer is

Table 1
Summary of samples, pretreatment, selenate and uranyl concentrations. The first letter in the sample name indicates the type or pretreatment, the first number indicates the starting concentration of selenate and the second number the uranyl concentration (N: polished iron foils, no precorrosion, P: iron foils precorroded for 300 d at 25 °C in 0.42 mM U(VI), UO_2: 1 g UO_2 powder, no iron).

Sample	Se(VI) [μM]	U(VI) [μM]	Time to XAS [d]	Conc at XAS Se/U [μM]	Final conc Se/U after 684 days [μM]
N-250Se/420U	250	420	20	13/<1	<1/<1
N-250Se	250	–	60	233/–	99/–
P-250Se	250	–	60	213/0.6	106/<1
P-250Se/420U	250	420	–	–	<1/<1
UO_2–250	250	–	–	–	239/–

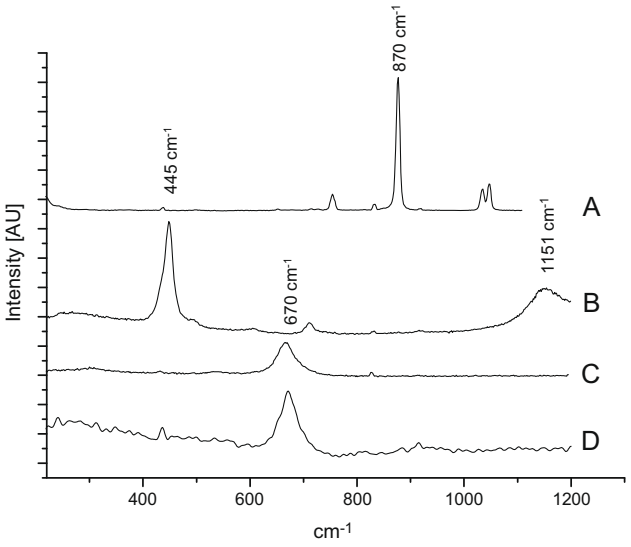

Fig. 1. Representative Raman spectra of the precorroded materials: (A) uranyl nitrate, (B) UO_2 powder, (C) magnetite powder and (D) iron foil precorroded in uranyl solution.

composed of magnetite. The bands at 445 cm^{-1} and 1151 cm^{-1} on the bulk UO_2 material are consistent with close to stoichiometric UO_2 [19] which was also confirmed by XRD. No uranium species could however be detected by Raman analysis on the iron foil precorroded in uranyl despite the immobilization of all uranyl from solution and the appearance of black corrosion products covering the surface. We can only speculate that otherwise clear Raman bands of cubic UO_2 disappear with structural disorder and that the uranium species on the precorroded foil could likely be amorphous or nanoparticulate UO_2 with little to no Raman signal. Dark coloured corrosion products also absorb more of the laser light making Raman analysis difficult. Comparing with the uranyl nitrate reference (Fig. 1) no adsorbed uranyl (UO_2^{2+} ~870 cm^{-1}) can be detected on the surface of the foil.

3.2. BET

The BET-surface area of a larger parallel batch of precorroded foils was measured (Micromeritics Flowsorb II 2300, He/N_2: 70/30). The detection limit of the instrument is ~0.1 m^2. Due to this limitation approximately 10 times more material than what was used in the actual experimental samples was used for the BET-area measurement of the polished foils with no precorrosion, N that did not show any detectable BET-area (<0.01 m^2). The bulk UO_2 powder equivalent to sample UO_2–250Se has the BET-area of 5.85 m^2 (corresponding to 5.85 m^2/g). U-precorroded foils equivalent to sample P-250Se yielded a BET-area of ~0.72 m^2.

3.3. Dynamics of immobilization

The concentrations of Se and U in the experimental solutions were measured as a function of reaction time (the analytical error is estimated to 1–10 μM). The results are displayed in Fig. 2(a) and (b). All solutions contained 10 mM NaCl and 2 mM $NaHCO_3$. The pH was measured and remained constant at ~7 for samples N-250Se/420U and P-250Se/420U and ~8 for samples, N-250Se, P-250Se, and UO_2–250Se during the course of all experiments.

The reference sample is a solution containing 10 mM NaCl, 2 mM NaHCO3, 0.25 mM selenate and 0.42 mM uranyl. The stable levels of Se and U of this solution indicate no or very limited sorption to the vessel or precipitation under the present conditions

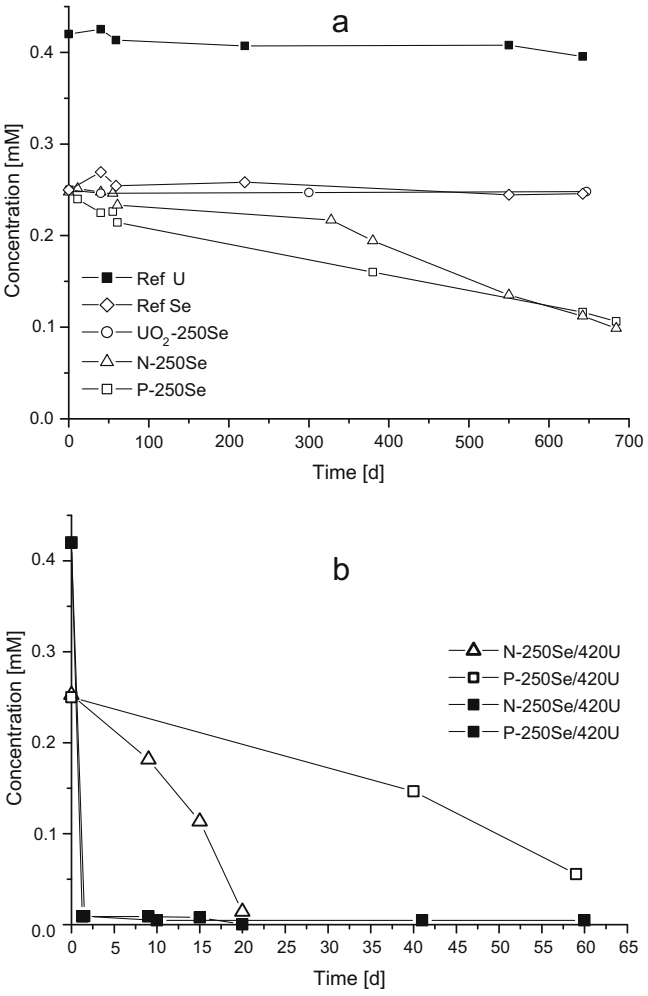

Fig. 2. (a–b) Immobilization dynamics of the samples. Open symbols represent Se-concentrations, closed symbols are U-concentrations.

(Fig. 2(a)). From the samples where a solid substrate is present we can see that the Se concentration decreases very slowly for the polished iron foil (sample N-250Se, Fig. 2(a)). The uranyl is almost completely consumed within 2 days by the materials. When uranyl and selenate are added simultaneously, the Se concentration decreases rapidly in the presence of a polished iron foil (sample N-250Se/420U). When a polished iron foil is pretreated with uranyl (300 days prior to the addition of selenate) only a slight increase in the initial rate of Se concentration reduction is observed (sample P-250Se, Fig. 2(a)) compared to the experiment where no uranyl was added. When more uranyl (which is very rapidly consumed) was added to the solution the rate of Se concentration reduction increased considerably (sample P-250Se/420U, Fig. 2(b)) reaching similar values as in sample N-250Se/420U, Fig. 2(b). No significant reduction in Se concentration was observed over 684 days in the pure UO_2 powder sample, UO_2–250Se (Fig. 2(b)). This indicates that the nature of the uranyl effect is transient and that bulk UO_2 itself is most likely not the active reagent. Comparing the rates of Se immobilization of P-250Se and N-250Se/420U which both have similar surface areas and UO_2–250Se which has a significantly larger BET-surface area the increase in surface area itself does not appear to govern the rate of Se-immobilization.

3.4. Characterization of the samples

The samples from the batch experiments were found to have a rather heterogeneous speciation. Raman spectroscopy indicates

the presence of the iron corrosion product magnetite (strong band at 670 cm^{-1}) on all iron containing samples and to a lesser degree maghemite and hematite. Evidence for a very heterogeneous spatial distribution of elemental Se was obtained for sample N-250Se/420U (Fig. 3) where the intensity of the band at 236 cm^{-1} (corresponding to the stretching mode of trigonal zero-valent Se [20], varied significantly between different spots. Raman bands at 236 cm^{-1}, evidence of elemental Se was also observed on sample P-250Se/420U (Fig. 4), as well as several iron oxides, the band at 670 cm^{-1} in the middle spectra is assigned to magnetite (Fig. 4), the broadened band at ~716 cm^{-1} is assigned to maghemite and the bands at 1308 and 296 cm^{-1} are assigned to hematite (Fig. 4).

Raman spectra from sample N-250Se (Fig. 5) also indicate significant presence of magnetite, maghemite and hematite. The strong band at 256 cm^{-1} in the middle spectra and partly in the lower spectra in Fig. 5 could be attributed to monoclinic or amorphous elemental selenium, or a mixed allotropy of elemental selenium [21,22].

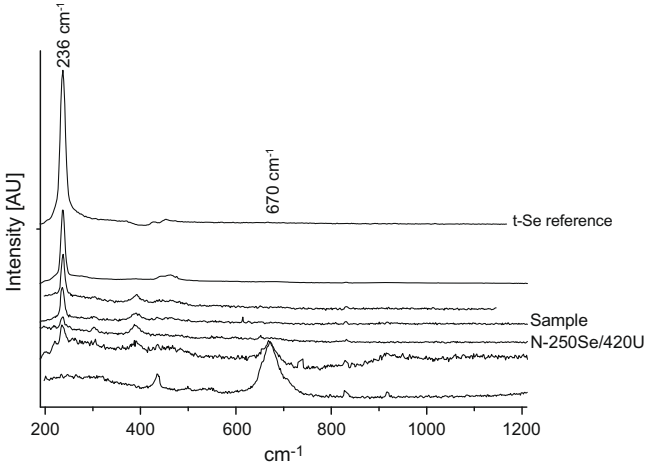

Fig. 3. Raman spectra of six random spots on sample N-250Se/420U and the elemental Se reference (upper spectra).

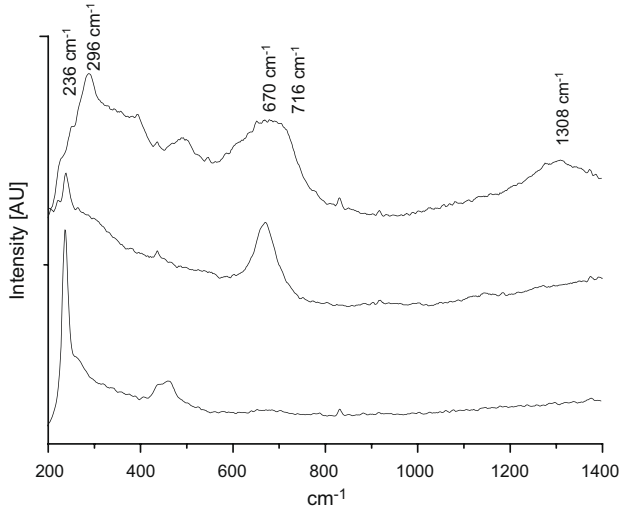

Fig. 4. Raman spectra from three spots on sample P-250Se/420U.

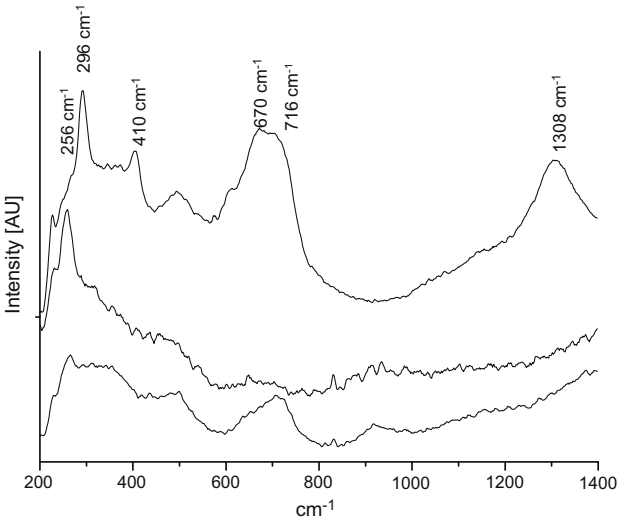

Fig. 5. Raman spectra from three spots on sample N-250Se.

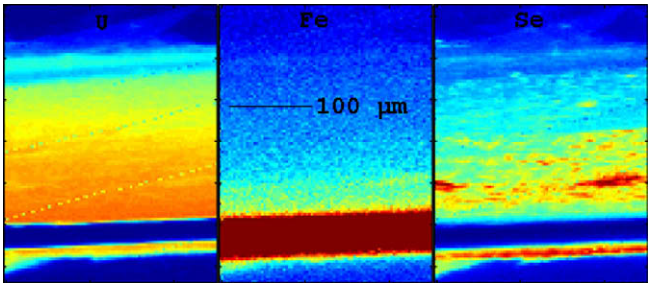

Fig. 6. U, Fe and Se µ-XRF-map of a cross section of sample N-250Se/420U. Red corresponds to high and blue to low concentrations (the diagonal dots are an artifact from the mapping sequence). (For interpretation of the references to colour in this figure legend, the reader is referred to the web version of this article.).

3.5. Elemental distribution

The elemental spatial distribution of Fe, U and Se was investigated with SEM–EDS and microprobe fluorescence mapping.

XRF and SEM–EDS scanning of sample N-250Se/420U revealed the presence of large amounts of Se and U. As can be seen in Fig. 6, the iron rich corrosion layer is extending a few µm from the cross section of the iron foil (20 µm initial foil thickness). Se rich regions appear to be associated with the edge of the iron corrosion front, mixed with uranium rich layers. The uranium layers on the top side of the foil extend over 100 µm from the iron foil and also appear to extend farther into the iron corrosion layer. The upper side in Fig. 5 with the thicker layers corresponds to the top side of the iron foil during the experiment. The foil was slightly bent to prevent the bottom side of the foil to be directly in contact with the vessel (not visible in Fig. 6). The conditions at the bottom side of the foil appear to have favored a sharper and thinner corrosion layer, particularly in the case of the thickness of the uranium layers. This could be due to the more limited exposure to the bulk solution or an effect of gravity given that the corrosion layers appeared to be loosely attached to the foil. As in the case of Raman spectroscopy, SEM–EDS analysis revealed a very heterogenous Se distribution on the sample, with micrometer sized hotspots of up to 40 atom-% Se. In sample P-250Se the uranium layers were more disrupted probably due to partial delamination of the thick layers during the long precorrosion time. Very little

Se was observed on sample N-250Se with isolated small hotspots a few μm in size containing <1% Se. No Se was detected on sample UO_2–250Se.

3.6. Micro XANES

Micro XANES (Micro X-ray Absorption Near Edge Structure) spectroscopy was employed to investigate the speciation of Se and U on the samples. Representative selenium micro XANES spectra from the three investigated samples and the bulk XANES spectra of reference compounds are presented in Fig. 7.

Using the energy of the absorption edge at half-height of the normalized XANES for the Se(VI), (IV), (0) and ferroselite, Se(-I) reference materials resulted in a perfectly linear correlation ($R^2 = 0.9996$) of the edge energy to the oxidation state. Assigned edge energies of samples and references can be found in Table 2. Definite assignment of the oxidation state of reduced Se species from XANES spectra is however difficult as a non linear relationship was observed for the oxidation state and edge energy of the dioctyldiselenide Se(-I) reference. This phenomenon has been observed in several XAS studies of reduced selenium [10,23–25]. The Se K edge has also been reported to be sensitive to varying degrees of crystallinity and different elemental allotropes [26]. The micro XANES Se spectra of the samples have the same general features and closely matching edge energies regardless if the maximum of the first derivative of the edge, the edge maxima or the energy of the absorption edge at half-height of the normalized XANES is used to assign the edge energy. The assigned edge energy for the samples can be found in Table 2. The selenium on the measured samples and in all spots (total of 25 spots) was found to be reduced to states close to or lower than Se(0) with no discernable difference in oxidation state between different spots and samples. Possible effects from overabsorption were investigated by changing the sample-detector geometry from 45° to 90°. However, no effects could be detected. XANES measurements were not performed on samples P-250Se/420U and UO_2–250Se.

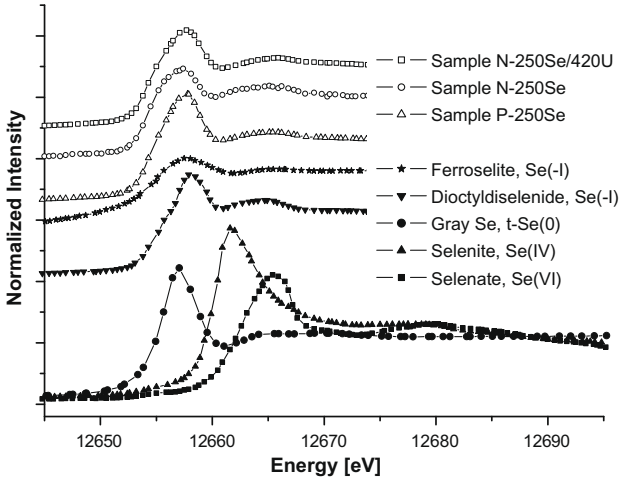

Fig. 7. Se-XANES spectra of the samples and references.

Table 2
Assigned edge positions based on the energy of the absorption edge at half-height of the normalized XANES spectra.

Sample	Se (eV)
Sodiumselenate, Se(VI)	12660.6
Sodiumselenite, Se(IV)	12658.5
Gray selenium, Se(0)	12653.8
Ferroselite, Se(-I)	12652.6
Dioctyldiselenide, Se(-I)	12654.3
N-250Se/420U	12653.8
N-250Se	12653.7
P-250Se	12653.9
Sample	**U (eV)**
Uranylnitrate, U(VI)	17168.8
UO_2, U(IV)	17164.4
N-250Se/420U	17164.4

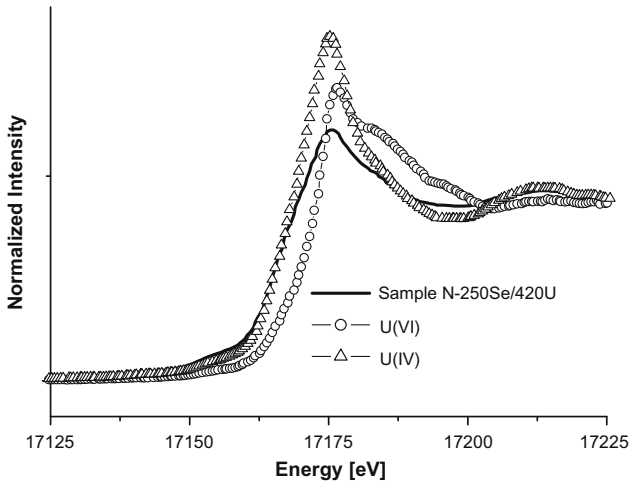

Fig. 8. Comparison of normalized U_L–XANES spectra of UO_2, $UO_2(NO_3)_2$ and uranium in sample N-250Se/420U.

The reduction of Se to states close to or lower than Se(0) is supported by the Raman band corresponding to elemental Se in samples N-250Se/420U and P-250Se/420U.

The speciation of the immobilized uranium was investigated using micro XANES for sample N-250Se/420U (Fig. 8). Linear combination fits, LCF of the experimental XANES spectra with spectra of U(IV) and U(VI) reference compounds indicates that the investigated uranium spots consisted of ~85% U(IV). The LCF fits were processed using the Labview software package from the Advanced Light Source beamline 10.3.2 [27].

As in the case of the Raman analysis of the iron foils precorroded in uranyl, no uranium species could be detected by Raman spectroscopy on any of the samples. Since thick layers (Fig. 5) of uranium largely reduced to U(IV) could be detected by U-XAS on sample N-250Se/420U we speculate that the immobilized uranium on the samples is largely reduced to amorphous or nanocrystalline UO_2. This is supported by the absence of any Raman bands that can be attributed to adsorbed uranyl (attempts to characterize the corrosion products by powder XRD were not successful).

As was observed in samples N-250Se/420U and P-250Se/420U the presence of uranyl being immobilized significantly increased the rate of selenate immobilization.

For sample N-250Se/420U the analysis shows that Se is close to completely reduced to Se(0) and that the uranium is largely reduced to U(IV). Considering the initial concentration ratio of U(VI) to Se(VI) of ~1.68 the rapid reduction of virtually all the Se(VI) to Se(0) cannot be explained solely by the formation of a non catalytic reactive corrosion product from the reduction of U(VI) in solution.

A hypothesis is that the reduction of uranyl by iron promotes the formation of a conducting iron oxide lowering the activation energy for reduction of Se(VI) by Fe(0).

Magnetite and green rusts (GR) have previously been identified as such conductive corrosion products capable of transferring

electrons from underlying elemental Fe to adsorbed species leading to (catalytic) reduction of the adsorbed species [18]. Magnetite was identified as a corrosion product in this study. However, sample P-250Se where a magnetite layer formed during the precorrosion in uranyl solution was very slow in immobilizing selenate, indicating that magnetite has a limited capacity to facilitate the reduction of selenate under the present conditions. It is possible that a transient reactive corrosion product is initially formed in sample P-250Se, but that the delay of ~300 days prior to addition of selenate provided sufficient time for the more reactive corrosion product to disappear. However when simultaneously adding uranyl and selenate to the system (sample P-250Se/420U) the precorroded surface quickly immobilized all the uranyl, accompanied by an increased rate of reductive immobilization of the selenate to Se(0) or lower. GR are non stoichiometric layered Fe(II)–Fe(III) hydroxy-salts that are well established as intermediate products during the corrosion of iron under anoxic conditions [28], sometimes accompanied by formation of magnetite as a product of GR oxidation [6]. Formation of GR is reported under conditions similar to those of this study [29]. No GR could however be identified in the Raman investigation, but the existence of transient GR corrosion products cannot be ruled out. The experimental observations suggest that presence of uranyl (and possibly other oxidants) being reduced by a corroding iron surface will enhance the rate of reduction of selenate under anoxic conditions, which is highly relevant for repository conditions.

Acknowledgements

The Swedish Nuclear Fuel and Waste Management Co (SKB) is gratefully acknowledged for financial support. Experimental assistance of the staff at the micro-XAS beamline, especially from Dr Daniel Grolimund and Dr Camelia Borca at the Swiss Light Source (SLS) is gratefully acknowledged. Thanks are extended to Professor Lars Engman at Uppsala University, Sweden for kindly providing the dioctyldiselenide reference material.

References

[1] C.-M. Zhou, Z.-D. Wu, Nucl. Sci. Technique. 17 (2006) 21.
[2] T. Beauwens, P.D. Cannière, H. Moors, L. Wang, N. Maes, Eng. Geol. 77 (2005) 285.
[3] SKB, Fuel and Canister Process Report for the Safety Assessment SR-Can, SKB Technical Report No. TR-06-22, Swedish Nuclear Fuel and Waste Management Co., Stockholm, 2006.
[4] A.P. Murphy, Indust. Eng. Chem. Res. 27 (1988) 187.
[5] Y. Zhang, J. Wang, C. Amrhein, W.T. Frankenberger Jr., J. Environ. Qual. 34 (2005) 487.
[6] S.C.B. Myneni, T.K. Tokunaga, G.E. Brown, Science 278 (1997) 1106.
[7] S.R. Qiu, H.F. Lai, M.J. Roberson, M.L. Hunt, C. Amrhein, L.C. Giancarlo, G.W. Flynn, J.A. Yarmoff, Langmuir 16 (2000) 2230.
[8] A.M. Scheidegger, D. Grolimund, D. Cui, J. Devoy, K. Spahiu, P. Wersin, I. Bonhoure, M. Janousch, J. Phys. IV: Proc. 104 (2003) 417.
[9] R. López de Arroyabe Loyo, S.I. Nikitenko, A.C. Scheinost, M. Simonoff, Environ. Sci. Technol. 42 (2008) 2451.
[10] A.C. Scheinost, L. Charlet, Environ. Sci. Technol. 42 (2008) 1984.
[11] E.J. O'Loughlin, S.D. Kelly, R.E. Cook, R. Csencsits, K.M. Kemner, Environ. Sci. Technol. 37 (2003) 721.
[12] B. Grambow, E. Smailos, H. Geckeis, R. Muller, H. Hentschel, Radiochim. Acta 74 (1996) 149.
[13] A.M. Scheidegger, D. Grolimund, M. Harfouche, M. Willimann, B. Meyer, R. Dähn, D. Gavillet, M. Nicolet, P. Heimgartner, NEA Publication No. 6046 (2006) 81.
[14] L. Syper, J. Mlochowski, Synthesis 5 (1984) 439.
[15] T. Ressler, J. Synchrotron Radiat. 5 (1998) 118.
[16] D.L.A. De Faria, S. Venâncio Silva, M.T. De Oliveira, J. Raman Spectrosc. 28 (1997) 873.
[17] N.R. Smart, D.J. Blackwood, L. Werme, SKB-Technical Report TR-01–22 (2001).
[18] K. Ritter, M.S. Odziemkowski, R.W. Gillham, J. Contam. Hydrol. 55 (2002) 87.
[19] D. Manara, B. Renker, J. Nucl. Mater. 321 (2003) 233.
[20] V. Poborchii, A. Kolobov, K. Tanaka, Appl. Phys. Lett. 72 (1998) 1167.
[21] V. Poborchii, A. Kolobov, H. Oyanagi, S. Romanov, K. Tanaka, Nanostruct. Mater. 10 (1998) 427.
[22] Q. Li, V. Wing-Wah Yam, Chem. Commun. (2006) 1006.
[23] A. Ryser, D. Strawn, M. Marcus, J. Johnson-Maynard, M. Gunter, G. Möller, Geochem. Trans. 6 (2005) 1.
[24] E. Hullenbusch, F. Farges, M. Lenz, P. Lens, G. Brown, AIP Conf. Proc. 882 (2007) 229.
[25] M. Lenz, E.D. Van Hullenbusch, F. Farges, S. Nikitenko, C.N. Borca, P.N.L. Lens, Environ. Sci. Technol. 42 (2008) 7587.
[26] I.J. Pickering, G.E. Brown, T.K. Tokunaga, Environ. Sci. Technol. 29 (1995) 2456.
[27] M. Marcus, A.A. MacDowell, R. Celestre, A. Manceau, T. Miller, H.A. Padmore, R.E. Sublett, J. Synchrotron Radiat. 11 (2004) 239.
[28] I.R. McGill, B. McEnaney, D.C. Smith, Nature 259 (1976) 200.
[29] D. Cui, K. Spahiu, Radiochim. Acta 90 (2002) 623.